(14) M. S. Fischer, D. H. Templeton, A. Zalkin, and M. Calvin, *J. Am. Chem. Soc.*, **93**, 2622 (1971). Pc = phthalocyanine.

(15) R. Timkovich and A. Tulinsky, *J. Am. Chem. Soc.*, **91**, 4430 (1969). TPP = *meso*-tetraphenylporphyrin.

(16) This compound was obtained as a green amorphous solid according to the Grignard method;[10] it could not be induced to crystallize. Anal. Calcd for $C_{36}H_{48}N_4OMg$: C, 72.65; H, 7.96; N, 9.42. Found: C, 72.00; H, 8.47; N, 9.22. λ_{max} ($CHCl_3$), nm (log ϵ_{max}): 410 (5.30), 514 (3.53), 547 (3.71), 583 (3.80), 625 (4.37).

(17) C. B. Storm and A. H. Corwin, *J. Org. Chem.*, **29**, 3700 (1964). Etio II = etioporphyrin II.

(18) E. B. Fleischer and T. S. Srivastava, *J. Am. Chem. Soc.*, **91**, 2403 (1969); A. B. Hoffman, D. M. Collins, V. W. Day, E. B. Fleischer, T. S. Srivastava, and J. L. Hoard, *ibid.*, **94**, 3620 (1972); C. Maricondi, W. Swift, and D. K. Straub, *ibid.*, **91**, 5205 (1969).

(19) G. N. La Mar, G. R. Eaton, R. H. Holm, and F. A. Walker, *J. Am. Chem. Soc.*, **95**, 63 (1973).

(20) W. M. Reiff, W. A. Baker, Jr., and N. E. Erickson, *J. Am. Chem. Soc.*, **90**, 4794 (1968). salen = *N,N'*-ethylenebis(salicylidenimine).

(21) I. A. Cohen, *J. Am. Chem. Soc.*, **91**, 1980 (1969).

(22) H. J. Schugar, G. R. Rossman, C. G. Barraclough, and H. B. Gray, *J. Am. Chem. Soc.*, **94**, 2683 (1972).

(23) R. B. Woodward and V. Skaric, *J. Am. Chem. Soc.*, **83**, 4676 (1961).

(24) H. Ogoshi, N. Masai, Z. Yoshida, J. Takemoto, and K. Nakamoto, *Bull. Chem. Soc. Jpn.*, **44**, 49 (1971).

(25) J. J. Katz, G. L. Closs, E. C. Pennington, M. T. Thomas, and H. H. Strain, *J. Am. Chem. Soc.*, **85**, 3801 (1963).

(26) D. W. Thomas and A. E. Martell, *J. Am. Chem. Soc.*, **81**, 5111 (1959).

(27) H. Ogoshi and Z. Yoshida, *Bull. Chem. Soc. Jpn.*, **44**, 1722 (1971).

(28) H. Ogoshi, Y. Saito, and K. Nakamoto, *J. Chem. Phys.*, **57**, 4194 (1972).

(29) J. Kincaid and K. Nakamoto, *J. Inorg. Nucl. Chem.*, in press.

(30) L. J. Boucher and J. J. Katz, *J. Am. Chem. Soc.*, **89**, 1340 (1967).

(31) A. Earnshaw, "Introduction to Magnetochemistry", Academic Press, London, 1968.

(32) P. George, J. Beetlestone, and J. S. Griffith, *Rev. Mod. Phys.*, **36**, 441 (1964); M. Zerner, M. Gouterman and H. Kobayashi, *Theor. Chim. Acta*, **6**, 363 (1966); P. O'D Offenhartz, *J. Chem. Phys.*, **42**, 3566 (1965); W. A. Eaton and R. M. Hochstrasser, *ibid.*, **49**, 985 (1968); H. Ogoshi, E. Watanabe, and Z. Yoshida, *Chem. Lett.*, 989 (1973).

(33) M. S. Fischer, D. H. Templeton, A. Zalkin, and M. Calvin, *J. Am. Chem. Soc.*, **94**, 3613 (1972).

(34) R. C. Pettersen, *Acta Crystallogr., Sect. B*, **25**, 2527 (1969).

(35) R. C. Pettersen, *J. Am. Chem. Soc.*, **93**, 5629 (1971).

(36) M. Zerner and M. Gouterman, *Theor. Chim. Acta*, **4**, 44 (1966); **8**, 26 (1967); G. M. Maggiora, *J. Am. Chem. Soc.*, **95**, 6555 (1973).

(37) J. L. Hoard, *Science*, **174**, 1295 (1971).

Contribution from the Gibbs Chemical Laboratory,
Harvard University, Cambridge, Massachusetts 02138

Studies on the Thermal Rearrangements of Chlorophosphacarboranes. Molecular and Crystal Structure of 9,10-Dichlorophosphacarborane

HOU S. WONG and WILLIAM N. LIPSCOMB*

Received July 16, 1974 AIC40481+

Thermal rearrangement at 450° of 12-chloro-1,2-phosphacarborane gave almost exclusively 9(10)-chloro-1,7-phosphacarborane as the product. The molecular and crystal structure of 9,10-dichloro-1,7-phosphacarborane (9,10-Cl_2-1,7-$CHPB_{10}H_8$) has been determined. This compound crystallizes in the space group $P2_1/n$. Unit cell parameters are a = 7.216 (2) Å, b = 12.468 (4) Å, c = 12.008 (3) Å, and β = 93.34 (2)°, with four molecules per unit cell. Intensity data were collected on a Picker FACS-1 diffractometer. The structure was solved by the conventional heavy-atom method. The final value of $R_F = \sum ||k|F_o| - |F_c||/\sum k|F_o|$ is 0.081 for 1342 independent X-ray diffraction maxima. The chlorine substitutions at the 9 and 10 positions are confirmed. As expected, the phosphorus atom is found to introduce significant distortion in the icosahedral structure. The six 1,7- and two 1,12-monochlorophosphacarborane isomers are isolated and their rearrangements at 550° studied. Identifications of these isomers are based on the above structure determination, the respective VPC retention times, point group symmetries, and ^{11}B NMR. The initial, intermediate, as well as final yields of these rearrangements suggest a marked shift from the predominantly cuboctahedral rearrangement suggested by previous experiments on halocarboranes to one which may involve the rotation of pentagonal pyramids. Other alternative but less plausible mechanisms cannot yet be excluded.

Studies on the thermal rearrangements of both mono- and dihalocarboranes[1-3] of the icosahedral type have so far quite consistently supported the original proposal of a cuboctahedral intermediate,[4] including allowance for rotation of triangular faces in the cuboctahedron.[1-3] The other two major pathways that have been proposed involve either the rotation of a triangular face[5] of the icosahedron or, as proposed by Hawthorne,[6] the mutual rotation of two pentagonal pyramids of the icosahedron (Figure 1). Neither has been found to occur to any significant extent in the rearrangements of icosahedral carboranes.

Of the numerous isoelectronic analogs of the carborane(12) family, the phosphacarborane, $CHPB_{10}H_{10}$, in which a CH group has been replaced by an unsubstituted P atom (having an external lone pair) is a close relative. Its numbering scheme is shown in Figure 2, where the C atom is in the 1 position and the P atom is at the 2, 7, and 12 positions, respectively, in the three possible isomers. The asymmetry results in the possible existence of six 1,2-, six 1,7-, and two 1,12-$CHPB_{10}H_9X$ isomers. We therefore thought it might be interesting to study internal rearrangements similar to those of halocarboranes but with the possibility of subtle to drastic changes in the preferred mechanism caused by the presence of P as a heteroatom.

Experimental Section

Synthesis and Isolation of the Isomers. The $CHPB_{10}H_9Cl$ isomers were prepared by known procedures,[7] and 1,7-$CCH_3PB_{10}H_{10}$ was made by Todd's method.[8] Isolation of individual isomers was achieved by TLC on E&M precoated silica gel plates and preparative VPC on an F&M 720 temperature-programmed gas chromatograph: a $^1/_4$ in. × 8 ft Carbowax 20-M column operating between 175 and 225° was used for the final isolation. The 9,10-Cl_2-1,7-$CHPB_{10}H_8$ was prepared both from direct electrophilic chlorination of 1,7-$CHPB_{10}H_{10}$ and from electrophilic chlorination of isomer H (vide infra). It was purified by sublimation and recrystallization from *n*-heptane.

Thermal Rearrangements. Samples of about 5 mg of each isomer were sealed under vacuum in Pyrex tubes of about 5-ml volume. These were then placed in a muffle furnace set at the desired temperature. They were removed and quickly cooled after appropriate periods. Isomerization products were analyzed on a $^1/_8$ in. × 8 ft Carbowax 20-M column operating from 125 to 225°. Due to the large number of overlapping peaks, the peak areas were estimated by weighing the

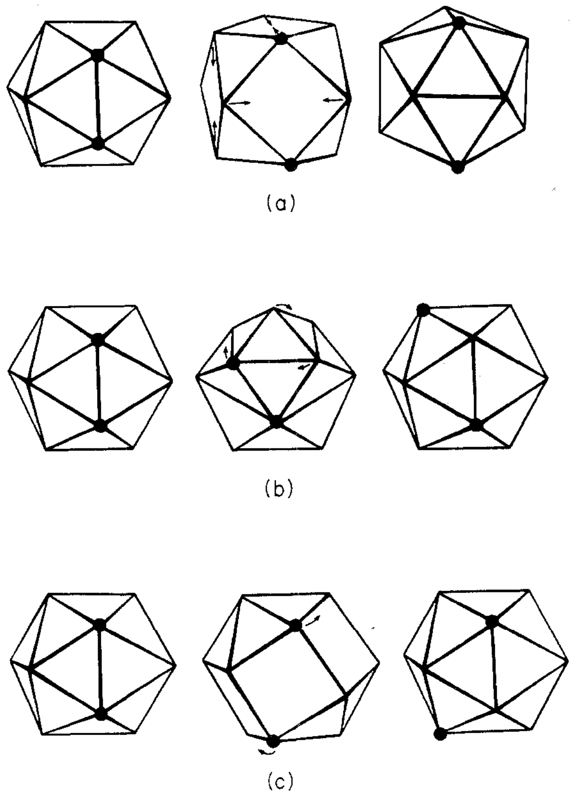

Figure 1. (a) Icosahedral rearrangement through the cuboctahedral intermediate. Triangle rotations occur within the cuboctahedral intermediate in rearrangements of halocarboranes. (b) Triangle rotation in the icosahedral unit. (c) Mutual rotation of two opposite pentagonal pyramids in the icosahedron.

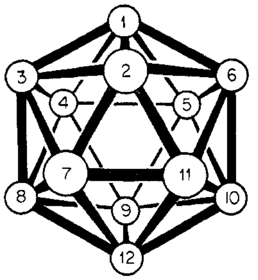

Figure 2. Numbering convention for the icosahedron.

appropriate peaks from the chromatograms. These determinations were at least duplicated and were accurate to 2%.

^{11}B NMR Spectra. All 80.53-MHz ^{11}B NMR spectra were recorded by Dr. R. J. Wiersema and C. Salentine at the University of California at Los Angeles. The solvent was $CHCl_3$, and all chemical shifts are referenced to $BF_3{\cdot}OEt_2 = 0$.

Calculation of Yields. The predicted percentage yields from the three major mechanisms were calculated with a program written by R. Bau and revised by H. Hart for the IBM 360 computer.

Mass Spectra. All mass spectra were recorded on an AEI MS-9 mass spectrometer.

Crystal Structure. Unit Cell and Space Group. The electrophilic dichlorination product of 1,7-$CHPB_{10}H_{10}$ or the identical monochlorination product of isomer H (vide infra) was recrystallized from CH_2Cl_2 by slow evaporation at 20°. Large hexagonal plates thus obtained were cut into cubes and mounted inside glass capillaries which were then sealed to prevent sublimation

Weissenberg photographs of the $0kl$ and $1kl$ levels and precession photographs of the $h0l$, $h1l$, $hk0$, and $hk1$ levels showed Laue symmetry C_{2h}-$2/m$. The extinctions of $h0l$ when $h + l$ is odd and of $0k0$ when k is odd are consistent with the space group $P2_1/n$. A least-squares fit of a total of 27 high-angle reflections gave cell parameters of $a = 7.216$ (2) Å, $b = 12.468$ (4) Å, $c = 12.008$ (3) Å, and $\beta = 92.34$ (2)°. Assumption of four molecules per unit cell gave a calculated density of 1.42 g/cm^3 which agrees very well with the experimental value of 1.41 (2) g/cm^3 determined by the flotation method.

Collection and Reduction of Data. Intensity data were collected up to $2\theta = 120.0°$ from a Picker automated diffractometer using Cu Kα (1.542 Å) radiation filtered through Ni foil. An ω scan over 2.2° with a scan rate of 1°/min was used with stationary background counts before and after each scan. A takeoff angle of 3.0° and 1-mm collimators for both incident and diffracted beams were used. Three strong standard reflections were monitored at 50-reflection intervals. A small but steady decline of all three occurred over the data collection period amounting to about 7% of the original intensities. Two crystals were used to collect identical asymmetric units of data; both were mounted with the unique b axis along the goniometer axis.

Because of the sizable linear absorption coefficient, $\mu = 63.3$ cm^{-1}, and the larger than optimum dimensions of the crystals that had to be used (0.30 × 0.31 × 0.37 and 0.42 × 0.46 × 0.34 mm), we used a gaussian quadrature numerical integration method for calculating absorption corrections.[9] The transmission coefficients ranged from 0.254 to 0.369 for the first crystal and from 0.123 to 0.296 for the second.

Data from these two crystals, comprising two asymmetric units, were placed on a common scale by Rae's method.[10] The correlation as given by

$$R = \sum_{H,i} |S_i I_{H,i} - \bar{I}_H| / \sum_{H,i} \bar{I}_H = 0.043$$

where H is hkl, $I_{H,i}$ is the intensity of reflection H in data set i, $\bar{I}_H$ is the average value of reflection H, and S_i is the scale factor for set i. Several reflections that were victimized by extinction were removed. The final data set comprised 1342 independent reflections for which $I > 2\sigma(I)$, where

$$\sigma(I) = [C + (T_c/2T_b)^2(B_1 + B_2)]^{1/2}$$

and where C is the total count of the scan, B_1 and B_2 are background counts, T_c is the total scan time, and T_b is the single background scan time.

Structure Determination and Refinement

A three-dimensional Patterson map contained two more than the expected number of peaks on the Harker plane at $v = 1/2$. Two of the heavy atoms were subsequently found to have nearly identical y coordinates from the Harker line at $(1/2, v, 1/2)$. All three heavy atoms were then located unambiguously from the interatomic vectors. A structure factor calculation phased by these atoms (all assumed to be chlorines at this point) yielded

$$R_F = \sum_{hkl} |k|F_o| - |F_c|| / \sum_{hkl} k|F_o| = 0.425$$

where temperature and scale factors were taken from the Wilson plot.

A three-dimensional electron density map then clearly indicated the positions of all of the remaining 11 cage atoms. At this stage these 11 atoms were introduced as boron into the calculations. The full-matrix refinement of scale factor, positional, and isotropic thermal parameters with half-shifts gave $R_F = 0.142$. The heavy atom making up one vertex of the icosahedron was identified as phosphorus by its large thermal parameter compared to the other two heavy atoms. This identification was also aided by chemical knowledge of the cage composition. Several more cycles of full-shift refinement of the atoms converged to $R_F = 0.125$. At this point, the carbon atom was clearly differentiated from the other cage borons by its smaller thermal parameter and shorter intercage bond distances.

Anisotropic thermal parameter refinement of the now correctly identified nonhydrogen atoms led to $R_F = 0.093$. A difference electron density map at this stage revealed all nine cage hydrogens, which were subsequently included in the structure factor calculations but were not further refined. All hydrogens were assigned isotropic temperature factors of the cage atoms to which they are bonded. Continued refinement of all positional and anisotropic thermal parameters for all nonhydrogen atoms then finally converged, yielding shifts of less than 0.25 for all parameters. The final value of R_F is 0.081 and of R_w is 0.028, where

$$R_w = [\Sigma w(k^2|F_o|^2 - |F_c|^2)^2 / \Sigma w(kF_o)^4]^{1/2}$$

Here, $w = 1/F_o{}^2$ for $F_o \geq 17.5$ and $w = (1/17.5)F_o$ for $F_o \leq 17.5$. The final value of the scale factor was 0.221 (4).

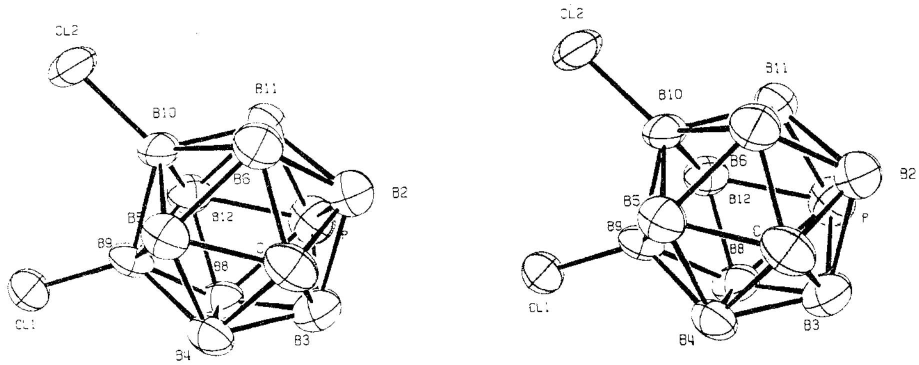

Figure 3. Stereoview of the structure of $9,10\text{-}Cl_2\text{-}1,7\text{-}CHPB_{10}H_8$.

Table I. Final Atomic Coordinates[a]

Atom	*x*	*y*	*z*
		I. Heavy Atoms	
Cl(1)	0.0665 (3)	0.0599 (2)	0.1314 (2)
Cl(2)	0.3403 (3)	0.0514 (2)	0.3927 (2)
C	0.0570 (11)	0.3625 (7)	0.3248 (7)
B(2)	−0.0341 (15)	0.3329 (8)	0.4492 (9)
B(3)	−0.1765 (15)	0.3362 (9)	0.3181 (9)
B(4)	−0.0371 (13)	0.2906 (8)	0.2134 (7)
B(5)	0.1912 (12)	0.2574 (8)	0.2742 (8)
B(6)	0.1823 (13)	0.2823 (8)	0.4191 (9)
P	−0.2423 (3)	0.2252 (2)	0.4311 (2)
B(8)	−0.1994 (13)	0.2009 (8)	0.2684 (9)
B(9)	0.0282 (13)	0.1526 (8)	0.2400 (8)
B(10)	0.1589 (13)	0.1494 (7)	0.3698 (8)
B(11)	0.0245 (14)	0.1936 (8)	0.4790 (8)
B(12)	−0.0762 (13)	0.1108 (8)	0.3661 (9)
		II. Hydrogen Atoms[b]	
HC	0.1027	0.4473	0.3104
HB(2)	−0.2961	0.4045	0.2966
HB(3)	−0.0481	0.3986	0.5123
HB(4)	0.3200	0.3087	0.4727
HB(5)	0.3329	0.2674	0.2214
HB(6)	−0.0156	0.3238	0.1192
HB(8)	0.0019	0.1599	0.5741
HB(11)	−0.3342	0.1736	0.2125
HB(12)	−0.1232	0.0189	0.3798

[a] Estimated standard deviations, shown in parentheses, refer to the last digit of the preceding number. [b] Coordinates from difference Fourier map, included but not refined in final least-squares cycles.

Table II. Anisotropic Thermal Parameters ($\times 10^4$)[a]

Atom	β_{11}	β_{22}	β_{33}	β_{12}	β_{13}	β_{23}
Cl(1)	219 (5)	70 (2)	60 (2)	6 (5)	−29 (5)	−31 (3)
Cl(2)	196 (4)	72 (2)	89 (2)	95 (5)	−88 (5)	−10 (3)
C	196 (17)	69 (6)	53 (6)	−62 (18)	−7 (18)	−9 (18)
B(2)	247 (26)	64 (7)	70 (8)	48 (23)	−45 (23)	−28 (14)
B(3)	212 (24)	75 (8)	81 (8)	71 (22)	−51 (23)	−4 (15)
B(4)	167 (21)	77 (8)	42 (6)	−3 (21)	25 (19)	13 (12)
B(5)	151 (19)	63 (8)	56 (7)	−26 (20)	15 (20)	4 (13)
B(6)	174 (20)	63 (7)	60 (7)	−19 (20)	−19 (20)	−10 (12)
P	171 (5)	93 (2)	82 (2)	−1 (6)	45 (5)	−9 (4)
B(8)	150 (19)	76 (7)	75 (8)	28 (20)	−29 (21)	23 (13)
B(9)	168 (18)	59 (6)	41 (7)	−41 (19)	−50 (18)	−6 (11)
B(10)	171 (20)	50 (7)	54 (7)	26 (19)	−68 (19)	−11 (11)
B(11)	177 (21)	64 (7)	51 (7)	6 (19)	20 (20)	3 (12)
B(12)	189 (21)	59 (7)	67 (8)	−19 (21)	−23 (21)	7 (13)

[a] Anisotropic thermal parameters are of the form $\exp[-(h^2\beta_{11} + k^2\beta_{22} + l^2\beta_{33} + hk\beta_{12} + hl\beta_{13} + kl\beta_{23})]$. Standard deviations are the same as in footnote *a* of Table I.

Table III

a. Interatomic Distances[a]

Bond	Dist, Å	Bond	Dist, Å
Cl(1)–Cl(2)	3.716 (3)	B(3)–B(4)	1.74 (1)
Cl(1)–B(9)	1.803 (9)	B(8)–B(4)	1.76 (2)
Cl(2)–B(10)	1.772 (10)	B(8)–B(12)	1.83 (2)
B(10)–B(9)	1.79 (2)	B(6)–B(5)	1.82 (2)
B(10)–B(6)	1.81 (1)	B(6)–B(11)	1.77 (2)
B(10)–B(5)	1.79 (1)	B(5)–B(4)	1.77 (1)
B(10)–B(11)	1.80 (1)	B(11)–B(12)	1.83 (2)
B(10)–B(12)	1.80 (1)	B(2)–C	1.72 (1)
B(9)–B(8)	1.75 (2)	B(3)–C	1.70 (2)
B(9)–B(5)	1.79 (1)	B(6)–C	1.73 (2)
B(9)–B(4)	1.77 (1)	B(5)–C	1.75 (1)
B(9)–B(12)	1.76 (1)	B(4)–C	1.74 (2)
B(2)–B(3)	1.85 (2)	B(2)–P	2.01 (1)
B(2)–B(6)	1.74 (2)	B(3)–P	2.02 (1)
B(2)–B(11)	1.79 (2)	B(8)–P	2.03 (1)
B(3)–B(8)	1.82 (1)	B(11)–P	2.01 (1)
		B(12)–P	2.04 (1)

b. Average Bond Lengths

Bond type	No. averaged	Range,[a] Å	Av,[b] Å
B–Cl	2	1.77 (1)–1.80 (1)	1.79 (2)
B–P	5	2.01 (1)–2.04 (1)	2.02 (1)
B–C	5	1.70 (2)–1.75 (1)	1.73 (2)
B–B	20	1.74 (2)–1.85 (2)	1.79 (3)

[a] See footnote *a* of Table I. [b] Estimated standard deviations for average bond lengths were calculated using $\sigma^2 = \Sigma_{i=1}{}^n(x_i - \bar{x})^2/(N-1)$, where x_i is the *i*th bond length and $\bar{x}$ is the mean of the *N* equivalent bond lengths.

Results and Discussion

Crystal Structure. The final coordinates of the atoms and their standard deviations are given in Table I. Anisotropic thermal parameters are listed in Table II. Bond distances are in Table III, and bond angles are presented in Table IV. Interesting least-squares planes and dihedral angles are in Table V. Structure factors have been recorded and are available elsewhere.[11]

The crystal structure, shown in Figure 3, is a distorted icosahedron having C_s symmetry within two standard deviations. In each molecule, atom pairs Cl(1) and Cl(2), B(2) and B(3), B(4) and B(6), B(8) and B(11), and B(9) and B(10) are related by the noncrystallographic mirror plane made up of atoms C, B(5), B(12), and P. The chlorines are bound to the chemically equivalent B(9) and B(10) atoms.

The distortion of the cage from idealized icosahedral geometry in $9,10\text{-}Cl_2\text{-}1,7\text{-}CHPB_{10}H_8$ is due in a large part to the presence of the phosphorus atom. The average B–P bond length of 2.02 (1) Å is significantly longer than the B–C bonds at 1.73 (2) Å and B–B bonds at 1.79 (3) Å.

The icosahedral planes P–B(3)–B(4)–B(9)–B(12) and P–B(8)–B(9)–B(10)–B(11) show considerable deviations from planarity (Table Va). On the other hand, the "normal" icosahedral planes B(2)–B(3)–B(8)–B(12)–B(11) and B(4)–B(5)–B(10)–B(12)–B(8) are planar within experimental error. The dihedral angles between the sets of planes P–B(2)–B(3) and C–B(2)–B(3), P–B(3)–B(8) and B(4)–

Table IV. Interatomic Angles[a]

Atoms	Angle, deg	Atoms	Angle, deg
I. Angles around C and P Atoms			
B(2)-C-B(3)	65.5 (8)	B(2)-P-B(3)	54.5 (6)
B(2)-C-B(6)	60.6 (8)	B(2)-P-B(8)	94.5 (6)
B(2)-C-B(5)	113.3 (9)	B(2)-P-B(11)	53.0 (6)
B(2)-C-B(4)	113.9 (9)	B(2)-P-B(12)	93.7 (6)
B(3)-C-B(6)	114.5 (9)	B(3)-P-B(8)	53.5 (6)
B(3)-C-B(5)	112.4 (9)	B(3)-P-B(11)	93.5 (6)
B(3)-C-B(4)	60.7 (8)	B(3)-P-B(12)	93.4 (6)
B(6)-C-B(5)	63.2 (7)	B(8)-P-B(11)	93.7 (6)
B(6)-C-B(4)	112.6 (9)	B(8)-P-B(12)	53.5 (6)
B(5)-C-B(4)	61.0 (7)	B(11)-P-B(12)	53.7 (6)
II. Angles around B Atoms			
B(3)-B(2)-B(6)	106.9 (10)	B(9)-B(8)-B(3)	106.5 (9)
B(3)-B(2)-P	63.1 (7)	B(9)-B(8)-P	113.4 (8)
B(3)-B(2)-B(11)	107.6 (10)	B(9)-B(8)-B(4)	60.3 (8)
B(3)-B(2)-C	56.8 (8)	B(9)-B(8)-B(12)	58.9 (7)
B(6)-B(2)-P	115.0 (9)	B(3)-B(8)-P	63.1 (6)
B(6)-B(2)-B(11)	60.0 (8)	B(3)-B(8)-B(4)	57.9 (8)
B(6)-B(2)-C	60.0 (8)	B(3)-B(8)-B(12)	108.1 (9)
P-B(2)-B(11)	63.6 (7)	P-B(8)-B(4)	112.6 (8)
P-B(2)-C	111.0 (9)	P-B(8)-B(12)	63.6 (6)
B(11)-B(2)-C	105.8 (10)	B(4)-B(8)-B(12)	107.2 (9)
B(2)-B(3)-B(8)	107.9 (10)	B(10)-B(9)-B(8)	110.9 (9)
B(2)-B(3)-P	62.5 (7)	B(10)-B(9)-B(5)	60.2 (7)
B(2)-B(3)-B(4)	107.8 (10)	B(10)-B(9)-B(4)	108.2 (9)
B(2)-B(3)-C	57.7 (8)	B(10)-B(9)-B(12)	60.8 (7)
B(8)-B(3)-P	63.4 (6)	B(8)-B(9)-B(5)	109.6 (9)
B(8)-B(3)-B(4)	59.4 (8)	B(8)-B(9)-B(4)	60.2 (8)
B(8)-B(3)-C	106.6 (9)	B(8)-B(9)-B(12)	62.8 (8)
P-B(3)-B(4)	114.1 (9)	B(5)-B(9)-B(4)	59.8 (7)
P-B(3)-C	111.3 (8)	B(5)-B(9)-B(12)	109.9 (9)
B(4)-B(3)-C	60.8 (8)	B(4)-B(9)-B(12)	110.1 (9)
B(9)-B(4)-B(3)	109.6 (10)	B(9)-B(10)-B(6)	107.4 (9)
B(9)-B(4)-B(8)	59.5 (7)	B(9)-B(10)-B(5)	59.9 (7)
B(9)-B(4)-B(5)	60.8 (7)	B(9)-B(10)-B(11)	107.2 (9)
B(9)-B(4)-C	106.4 (9)	B(9)-B(10)-B(12)	58.9 (7)
B(3)-B(4)-B(8)	62.7 (8)	B(6)-B(10)-B(5)	60.7 (7)
B(3)-B(4)-B(5)	109.7 (10)	B(6)-B(10)-B(11)	58.7 (7)
B(3)-B(4)-C	58.5 (8)	B(6)-B(10)-B(12)	108.0 (9)
B(8)-B(4)-B(5)	109.9 (10)	B(5)-B(10)-B(11)	108.0 (9)
B(8)-B(4)-C	107.4 (9)	B(5)-B(10)-B(12)	108.2 (9)
B(5)-B(4)-C	60.0 (7)	B(11)-B(10)-B(12)	61.2 (8)
B(10)-B(5)-B(9)	59.9 (7)	B(10)-B(11)-B(2)	107.8 (10)
B(10)-B(5)-B(6)	60.0 (7)	B(10)-B(11)-B(6)	61.1 (7)
B(10)-B(5)-B(4)	107.6 (9)	B(10)-B(11)-P	114.4 (8)
B(10)-B(5)-C	104.9 (9)	B(10)-B(11)-B(12)	59.4 (7)
B(9)-B(5)-B(6)	106.8 (9)	B(2)-B(11)-B(6)	58.4 (8)
B(9)-B(5)-B(4)	59.4 (7)	B(2)-B(11)-P	63.4 (7)
B(9)-B(5)-C	104.6 (9)	B(2)-B(11)-B(12)	109.2 (10)
B(6)-B(5)-B(4)	106.6 (9)	B(6)-B(11)-P	113.5 (8)
B(6)-B(5)-C	57.7 (7)	B(6)-B(11)-B(12)	108.5 (9)
B(4)-B(5)-C	59.0 (7)	P-B(11)-B(12)	63.9 (6)
B(10)-B(6)-B(2)	109.8 (9)	B(10)-B(12)-B(9)	60.4 (7)
B(10)-B(6)-B(5)	59.2 (7)	B(10)-B(12)-B(8)	107.1 (9)
B(10)-B(6)-B(11)	60.3 (7)	B(10)-B(12)-P	113.2 (8)
B(10)-B(6)-C	105.4 (9)	B(10)-B(12)-B(11)	59.4 (7)
B(2)-B(6)-B(5)	109.0 (9)	B(9)-B(12)-B(8)	58.3 (7)
B(2)-B(6)-B(11)	61.6 (8)	B(9)-B(12)-P	112.3 (8)
B(2)-B(6)-C	59.4 (8)	B(9)-B(12)-B(11)	106.9 (9)
B(5)-B(6)-B(11)	108.0 (9)	B(8)-B(12)-P	62.9 (6)
B(5)-B(6)-C	59.2 (7)	B(8)-B(12)-B(11)	107.3 (9)
B(11)-B(6)-C	106.6 (9)	P-B(12)-B(11)	62.5 (6)
III. Angles Involving Cl Atoms			
Cl(1)-B(9)-B(10)	120.1 (8)	Cl(2)-B(10)-B(9)	122.3 (8)
Cl(1)-B(9)-B(8)	121.3 (8)	Cl(2)-B(10)-B(6)	122.5 (8)
Cl(1)-B(9)-B(5)	119.6 (8)	Cl(2)-B(10)-B(5)	121.5 (8)
Cl(1)-B(9)-B(4)	121.7 (9)	Cl(2)-B(10)-B(11)	122.0 (9)
Cl(1)-B(9)-B(12)	120.7 (9)	Cl(2)-B(10)-B(12)	121.6 (9)

[a] See footnote *a* of Table I.

B(3)–B(8), P–B(8)–B(12) and B(9)–B(8)–B(12) range from 144.5 to 145.7° (Table Vb) while those between "normal" triangle faces such as B(5)–B(9)–B(10) and B(9)–B(10)–B(12) and such as B(5)–B(4)–B(9) and B(4)–B(8)–B(9) range typically from 140.3 to 141.4°.

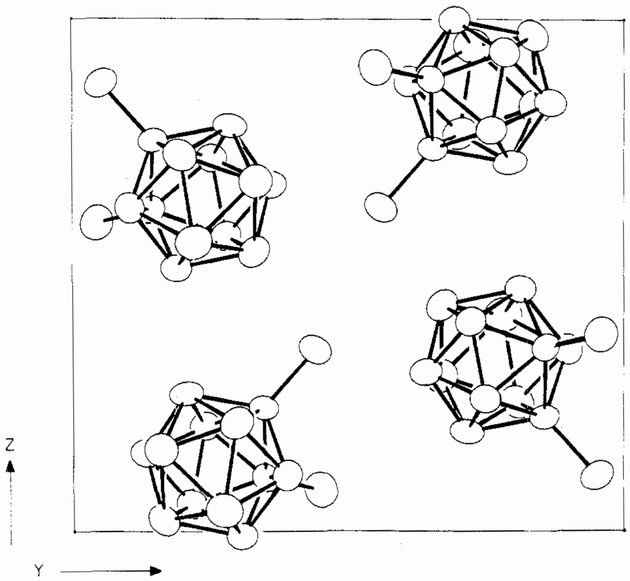

Figure 4. View of the unit cell packing of 9,10-Cl$_2$-1,7-CHPB$_{10}$H$_8$ by projection down the *a* or *x* axis.

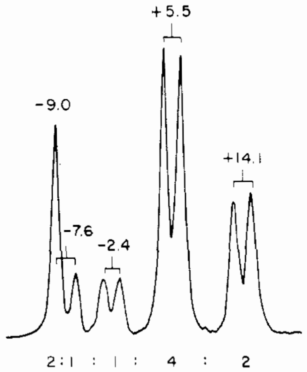

Figure 5. ^{11}B NMR spectrum of 9,10-Cl$_2$-1,7-CHPB$_{10}$H$_8$. Chemical shifts are relative to BF$_3$·OEt$_2$ = 0.

The distance of the P atom from the plane B(2)–B(3)–B(8)–B(12)–B(11) is 1.30 Å compared with the much shorter distance of B(9) from B(4)–B(5)–B(8)–B(10)–B(12) at 0.90 Å and of B(5) from the plane C–B(4)–B(9)–B(10)–B(6) at 0.97 Å. The B(2)–B(3)–B(8)–B(12)–B(11) pentagon is also enlarged with an average B–B distance of 1.82 Å when compared with the average distance of 1.78 Å between other borons on the cage.

A view of the packing in the unit cell is shown in Figure 4. Shortest intermolecular contacts are all greater than 2.69 Å, and no unusually small intermolecular distances are observed.

See Figure 5 for the ^{11}B NMR spectrum of 9,10-Cl$_2$-1,7-CHPB$_{10}$H$_8$.

The 1,2-CHPB$_{10}$H$_9$Cl Rearrangements. The radical chlorination of 1,2-CHPB$_{10}$H$_{10}$[7] gave four components which can be resolved by VPC (Figure 6a). Fractions J, K, and L were isolated and characterized by ^{11}B NMR. Comparison with the spectrum of the parent phosphacarborane 1,2-CHPB$_{10}$H$_{10}$ shows that while J and L are probably single isomers, K is obviously a mixture (Table VI). Since the two low-field doublets of area 1 (at −9.1 and −2.0 ppm) in 1,2-CHPB$_{10}$H$_{10}$ can only be assigned to B(9) or B(12), isomer L whose spectrum shows the collapse of one of these into a singlet can either be the 9- or 12-Cl isomer.

Furthermore, Zakharkin and Kyskin have suggested that the nonequivalence of the CH and trivalent P in phospha-

Table V

a. Least-Squares Icosahedral Planes[a]

Atom	Dev, Å	Atom	Dev, Å
Plane: P-B(3)-B(4)-B(9)-B(12) $0.1140X - 0.3454Y + 0.9315Z = 3.577$			
B(9)	+0.023	B(4)	+0.018
B(3)	−0.044	B(12)	−0.045
P	+0.048		
Plane: B(2)-B(3)-B(8)-B(12)-B(11) $-0.8535X - 0.1042Y + 0.5106Z = 2.725$			
B(2)	+0.006	B(11)	−0.002
B(3)	−0.009	B(12)	−0.004
B(8)	+0.008		
Plane: C-B(3)-B(8)-B(9)-B(5) $0.8021X + 0.3110Y + 0.5097Z = 3.636$			
B(9)	−0.021	B(5)	+0.038
B(3)	+0.028	C	−0.042
B(8)	−0.003		
Plane: P-B(8)-B(9)-B(10)-B(11) $0.2819X + 0.9499Y - 0.1346Z = 1.462$			
B(10)	−0.019	P	−0.045
B(9)	+0.018	B(11)	+0.041
B(8)	−0.040		
Plane: B(4)-B(5)-B(10)-B(12)-B(8) $-0.7205X + 0.6743Y - 0.1618Z = 0.747$			
B(10)	+0.008	B(4)	+0.013
B(8)	−0.008	B(12)	−0.000
B(5)	−0.013		
Plane: C-B(4)-B(9)-B(10)-B(6) $-0.8558X - 0.1298Y + 0.5007Z = 1.133$			
B(10)	−0.011	B(4)	−0.022
B(9)	+0.021	C	+0.016
B(6)	−0.022		
Plane: P-B(12)-B(5)-C $0.5087X - 0.0233Y + 0.8606Z = 3.383$			
B(5)	+0.007	B(12)	−0.006
C	−0.007	P	+0.006

b. Dihedral Angles between Triangle Faces

Triangle 1	Triangle 2	Dihedral angle, deg
P-B(2)-B(3)	C-B(2)-B(3)	144.5
P-B(3)-B(8)	B(4)-B(3)-B(8)	145.7
P-B(8)-B(12)	B(9)-B(8)-B(12)	144.8
B(5)-B(9)-B(10)	B(12)-B(9)-B(10)	140.3
B(5)-B(4)-B(9)	B(8)-B(4)-B(9)	141.4

[a] Planes are defined as $c_1X + c_2Y + c_3Z = D$, where *X, Y,* and *Z* are orthogonal coordinates (in Å) and axes parallel *a, b,* and *c**.

carboranes manifests itself in a higher positive charge on the C.[7] This conclusion is based on dipole moment measurements and on comparisons of the spectral intensities of the valence vibrations of the ir spectra of these compounds.[12,13] If it is then assumed that the VPC retention times of a $CHPB_{10}H_9Cl$ isomer depend on its dipole moment, a case experimentally verified in the analogous chloro- and bromocarboranes,[15,16] it is then possible to estimate the retention times of the $CHPB_{10}H_9Cl$ isomers.[7,12,13] These estimates are shown in Table VII. The tentative assignments for the 1,2 isomers result from correlations of VPC retention times, ^{11}B NMR, and point group symmetries. Isomer L is therefore assumed to be 12-Cl-1,2-$CHPB_{10}H_9$.

L was thermally rearranged at 450°. Very little of the other 1,2 isomers are produced during this isomerization, and the final product contains all six of the 1,7 isomers (Table VIII).

Table VI. 80.5-MHz ^{11}B NMR Spectra

	Chem shift[b]		Point group symmetry
Isomer	B-Cl[a]	B-H	
1,2-$CHPB_{10}H_{10}$		−9.1 (1), −2.0 (1), +1.6 (2), +7.8 (2), +8.8 (2), +12.7 (2)	C_s
J	−6.8 (1)	−11.1 (1), −8.7 (1), −2.0 (2), +3.2 (1), +4.0 (1), +7.5 (1), +9.9 (1), +11.5 (1)	C_1[c]
K	−14.3 (0.4) −9.1 (0.6)	−10.3 (0.6), −2.8 (0.6), −2.4 (0.4), +1.2 (0.8), +2.8 (0.6), +7.9 (2.4), +9.9 (1.6), +12.3 (0.6), +13.9 (0.8), +18.3 (0.6)	C_1[d]
L	−15.5 (1)	−13.5 (1), −2.8 (2), +4.8 (4), +9.5 (2)	C_s
1,7-$CHPB_{10}H_{10}$		−3.6 (1), +2.4 (1), +4.4 (2), +7.9 (4), +10.7 (2)	C_s
H	−6.4 (1)	−3.6 (1), +2.0 (1), +3.6 (1), +7.9 (2), +9.5 (2), +12.3 (1), +16.7 (1)	C_1
G	−9.8 (1)	−2.7 (1), +3.0 (2), +6.3 (2), +7.8 (2), +11.6 (2)	C_s
F	−6.3 (1)	−3.1 (1), −0.7 (1), +2.3 (1), +3.3 (1), +6.8 to +8.5 (3), +10.6 (1), +11.8 (1)	C_1
E	−9.4 (1)	+2.3 (1), +3.5 (2), +6.4 (2), +8.4 (2), +10.6 (2)	C_s
D	−2.9 (1)	−6.4 (1), +2.9 (3), +6.8 (2), +8.2 (1), +10.0 (1), +12.9 (1)	C_1
B	−1.1 (1)	−3.9 (1), +1.5 (1), +3.9 (2), +5.5 (2), +7.1 (2), +10.0 (1)	C_1
1,12-$CHPB_{10}H_{10}$		+7.2 (10)	C_s
C	−4.5 (1)	+6.3 (2), +8.6 (6), +14.5 (1)	C_s
A	−3.1 (1)	+5.0 to +6.6 (8), +12.4 (1)	C_s

[a] All B-Cl's are singlets. [b] Ppm relative to $BF_3 \cdot OEt_2 = 0$; the numbers in parentheses refer to the areas of the peaks. [c] The spectra of the 4(5)- and 7(11)-Cl-1,2 isomers appear to be coincident. [d] K is obviously a mixture.

Interconversion of the 1,7 isomers at 450° was tested and found to be absent. Intermolecular Cl exchange was also tested for. E.g., 1,7-$CCH_3PB_{10}H_{10}$ and isomer H were heated together for 24 hr at 450°; no evidence of the formation of either 1,7-$CHPB_{10}H_{10}$ or 1,7-$CCH_3PB_{10}H_9Cl$ was observed by VPC or mass spectral results.

The possibility still exists that H may be a product arising from a quasi steady state among the 1,2 isomers other than L. Tests showed that it was actually produced in much smaller amounts from either J or K (Table IX).

Thus it can be concluded that H arose mainly from L. The identity of H is suggested to be 9(10)-Cl-1,7-$CHPB_{10}H_9$ by its ^{11}B NMR spectrum; it has C_1 symmetry and also has the largest dipole moment of the 1,7 isomers (Figure 6c). This assignment is confirmed by the crystal and molecular structure determination of 9,10-Cl_2-1,7-$CHPB_{10}H_8$ described above. The tentative assignments for the other five 1,7 isomers are as presented in Table VII.

The 1,7- and 1,12-$CHPB_{10}H_9Cl$ Rearrangements. The electrophilic chlorination of 1,12-$CHPB_{10}H_{10}$ gives both possible isomers, A and C, with larger quantities of isomer C[7]

Table VII. Estimated Dipole Moments[a] and Tentative Assignments

Isomer	Dipole moment, D	Point group symmetry	Assignment
	I. $1,2\text{-CHPB}_{10}\text{H}_9\text{Cl}$		
12-Cl	5.5	C_s	L
9-Cl	5.3	C_s	K
8(10)-Cl	5.0	C_1	K
7(11)-Cl	4.4	C_1	J[b]
4(5)-Cl	4.0	C_1	J[b]
3(6)-Cl	3.3	C_1	I[c]
	II. $1,7\text{-CHPB}_{10}\text{H}_9\text{Cl}$		
9(10)-Cl	4.0	C_1	H
12-Cl	3.9	C_s	G
5-Cl	3.4	C_s	E
8(11)-Cl	3.2	C_1	F
4(6)-Cl	2.8	C_1	D
2(3)-Cl	1.3	C_1	B
	III. $1,12\text{-CHPB}_{10}\text{H}_9\text{Cl}$		
7-Cl	2.1	C_s	C
2-Cl	1.5	C_s	A

[a] Dipole moments are estimated from dipole moments of the parent phosphacarboranes and Cl-cage bond moments. The accuracy is about 10–15%. [b] Both 4(5)- and 7(11)-Cl-1,2 isomers gave identical VPC and ^{11}B NMR results. [c] I was not isolated nor characterized.

Table VIII. Isomerization of Isomer L at 450°

Time of rear-rangement, hr	%									
	$1,7\text{-CHPB}_{10}\text{H}_9\text{Cl}$						$1,2\text{-CHPB}_{10}\text{H}_9\text{Cl}$			
	B	D	E	F	G	H	I	J	K	L
2	0	0	0	0	0	7	0	0	4	89
4	0	0	0	0	4	27	0	0	4	65
20	2	2	2	5	13	77	0	0	0	0

Table IX. Final Yields (%) of $1,2\text{-CHPB}_{10}\text{H}_9\text{Cl}$ Rearrangements[a]

Starting isomer	B	D	E	F	G	H
J	26	22	27	16	5	4
K	24	28	11	20	4	13
L	2	2	2	5	13	77

[a] Yield after 24 hr at 450°.

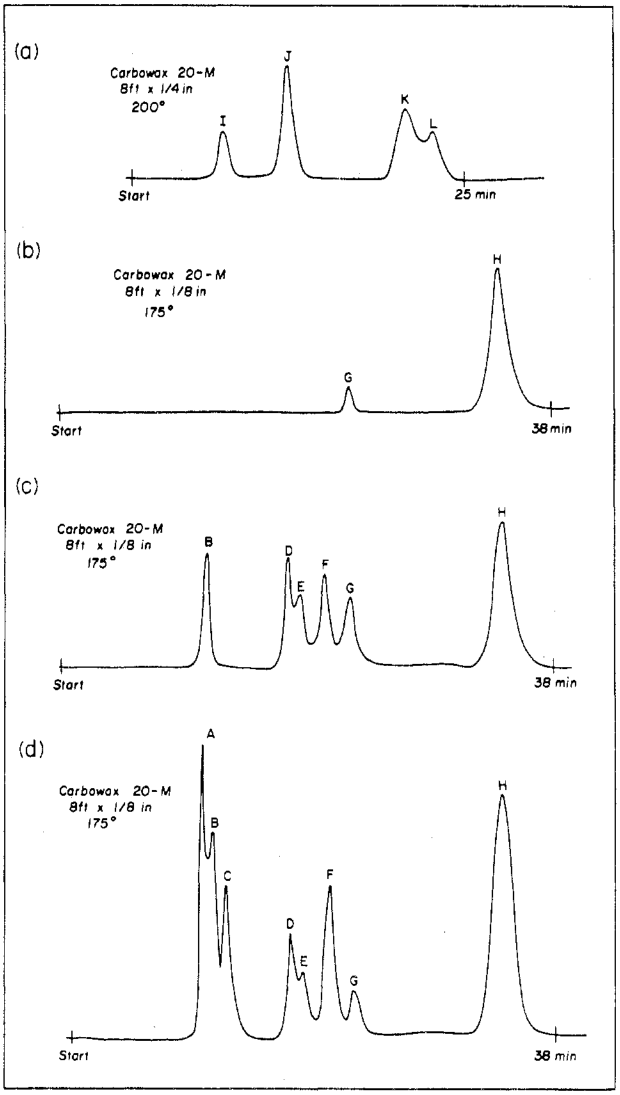

Figure 6. (a) VPC of the radical chlorination product of $1,2\text{-CHPB}_{10}\text{H}_{10}$. (b) VPC of the electrophilic chlorination product of $1,7\text{-CHPB}_{10}\text{H}_{10}$. (c) VPC of radical chlorination product of $1,7\text{-CHPB}_{10}\text{H}_{10}$. (d) VPC of the intermediate product of thermal isomerization of isomer H at 550°.

Table X. Initial Yield Percentages from the 1,7- and $1,12\text{-CHPB}_{10}\text{H}_9\text{Cl}$ Isomers

Starting isomer	Time at 550°, hr	B	D	F	E	G	H	A	C
B	0.5	26	12	17	5	0	3	3	3
	1.0	40	17	18	9	3	2	6	5
D	1.0	12	69	5	11	0	1	3	0
	4.0	15	24	12	17	1	5	21	5
F	1.0	25	8	51	3	2	5	1	5
E	1.0	8	8	7	64	0	4	8	1
G	4.0	2	1	4	1	76	3	1	13
	8.0	4	2	4	2	58	5	1	24
H	4.0	3	2	6	2	2	78	5	3
	8.0	7	5	8	3	2	60	10	5
A	3.0	2	5	3	7	0	5	78	1
	6.0	7	8	4	9	1	5	63	3
C	6.0	3	2	4	1	6	4	1	79
	12.0	5	6	7	7	9	8	7	51

which has the higher retention time. Consistent with dipole moment estimates, C is assigned to be 7-Cl- and A as 2-Cl-$1,12\text{-CHPB}_{10}\text{H}_9$.

These isomers and the six 1,7 isomers (see Figure 6c and d) were isolated as described and then rearranged at 550°. The profiles of initial yields are shown in Table X, and a typical intermediate VPC chromatogram is shown in Figure 6d.

All eight isomers gave nearly identical final yields after 48 hr at 550°, suggesting a final kinetic equilibrium. For example, H gave the final yields as shown.

Isomer	B	D	F	E	G	H	A	C
%	8	12	8	10	5	9	30	19

Intermolecular chlorine exchange was tested by heating a mixture of $1,7\text{-CCH}_3\text{PB}_{10}\text{H}_{10}$ and H at 550° for 24 hr; no formation of $1,7\text{-CCH}_3\text{PB}_{10}\text{H}_9\text{Cl}$ was detected by either VPC or mass spectral characterization of the product.

Mechanisms of the Rearrangements. The almost exclusive formation of 9(10)-Cl-$1,7\text{-CHPB}_{10}\text{H}_9$ from 12-Cl-$1,2\text{-CHPB}_{10}\text{H}_9$ can only arise in a single step from the mechanism based upon the rotation of pentagonal pyramids. The product of cuboctahedral rearrangement would have been the 12-Cl-1,7 isomer (G), whereas that predicted by pure triangle rotations on the icosahedral surface should have been equal amounts of both the 9(10)- and 12-Cl-1,7 isomers. Hence a drastic change in the rearrangement pathway compared to that in halocarboranes is implied.

The major trends in the initial yield profiles of these isomerizations provide a good indication of the mechanism in

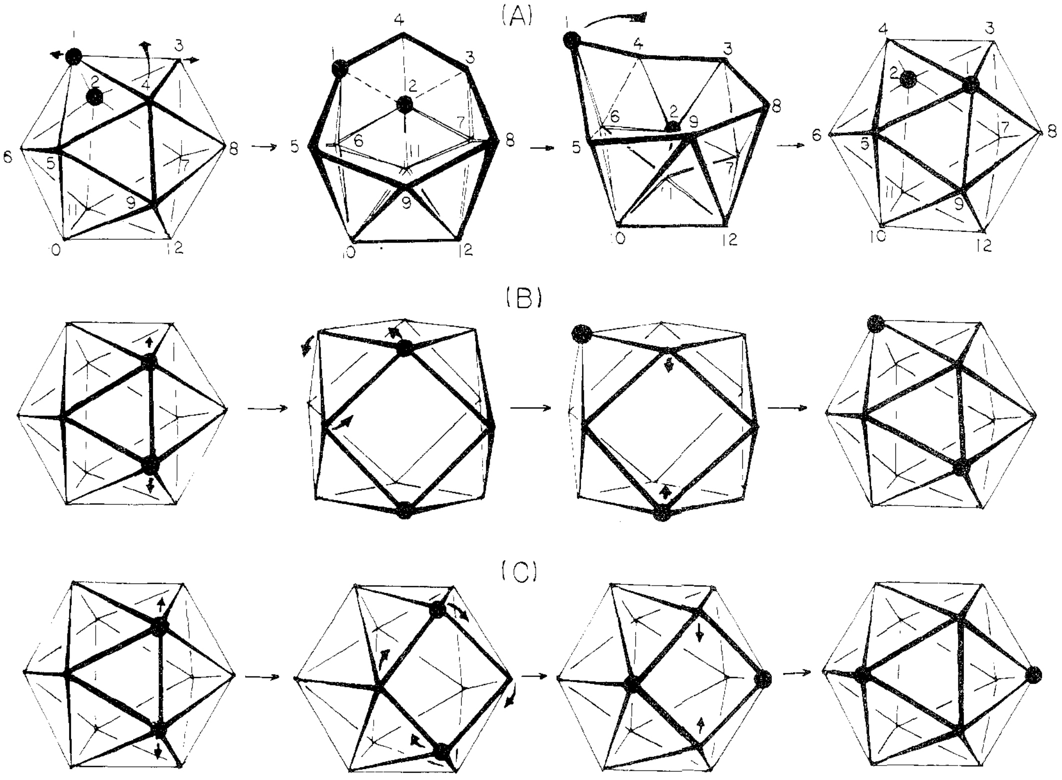

Figure 7. (A) Rearrangement through the pseudo 13-atom nido intermediate. (B) The cuboctahedron intermediate with selective rotation of triangles. (C) The diamond–square–diamond twist mechanism.

Table XI. Predicted Initial Yield Percentages from the Three Major Mechanisms[a]

Starting isomer	1,7-$\mathrm{CHPB_{10}H_9Cl}$ 2(3) B	4(6) D	8(11) F	5 E	12 G	9(10) H	1,12-$\mathrm{CHPB_{10}H_9Cl}$ 2 A	7 C
			I. Rotation of Pentagonal Pyramids[b]					
2(3)-Cl-1,7	75.8	4.0	4.0	0	0	0	9.7	6.5
4(6)-Cl-1,7	4.0	67.0	4.0	8.0	0	0	17.0	0
8(11)-Cl-1,7	4.0	4.0	67.0	0	8.0	0	0	17.0
5-Cl-1,7	0	10.8	0	74.9	0	3.5	10.8	0
12-Cl-1,7	0	0	10.8	0	74.9	3.5	0	10.8
9(10)-Cl-1,7	0	0	0	5.4	2.6	74.0	10.8	17.2
2-Cl-1,12	3.0	5.0	0	3.0	0	3.0	86.0	0
7-Cl-1,12	4.0	0	6.0	0	4.0	4.0	0	82.0
			II. Modified Cuboctahedron Intermediate[c]					
2(3)-Cl-1,7	73.1	16.7	8.3	0	0	2.0	0	0
4(6)-Cl-1,7	11.6	67.2	4.1	2.8	0	11.6	2.7	0
8(11)-Cl-1,7	11.6	4.1	67.2	0	2.8	11.6	0	2.7
5-Cl-1,7	0	3.1	0	93.2	0	1.0	2.7	0
12-Cl-1,7	0	0	3.1	0	93.2	1.0	0	2.7
9(10)-Cl-1,7	0.2	16.8	8.4	0.6	0.4	73.6	0	0
2-Cl-1,12	0	1.0	0	1.0	0	0	85.3	12.7
7-Cl-1,12	0	0	1.0	0	1.0	0	16.3	81.7
			III. Rotation of Triangle Faces[d]					
2(3)-Cl-1,7	62.5	16.7	8.3	0	0	0	7.5	5.0
4(6)-Cl-1,7	6.3	68.5	6.3	0	6.3	6.3	6.3	0
8(11)-Cl-1,7	6.3	6.3	68.5	0	6.3	6.3	0	6.3
5-Cl-1,7	0	12.5	0	74.9	0	6.3	0	6.3
12-Cl-1,7	0	0	12.5	0	74.9	6.3	6.3	0
9(10)-Cl-1,7	0	8.3	4.2	3.2	3.1	74.9	3.8	2.5
2-Cl-1,12	2.0	4.0	0	2.0	0	2.0	86.0	4.0
7-Cl-1,12	2.0	0	4.0	0	2.0	2.0	8.0	82.0

[a] All yields are adjusted to give a final ratio of 1,7 to 1,12 isomers of 1:1. [b] Equal probabilities were given to all pentagonal pyramids to rotate. [c] Equal probabilities for all triangles to rotate in the cuboctahedral intermediate were given. [d] All triangles were allowed to rotate on the icosahedron with equal probabilities.

operation. These trends from the 1,7 and 1,12 isomers are found to show the following characteristics: (1) the lack of conversion of 4(6)-Cl-1,7-$\mathrm{CHPB_{10}H_9}$ (D) into 9(10)-Cl-1,7-$\mathrm{CHPB_{10}H_9}$ (H), (2) the large conversion of D into 2-Cl-1,12-$\mathrm{CHPB_{10}H_9}$ (A), (3) the equal yields of D and A from 5-Cl-1,7-$\mathrm{CHPB_{10}H_9}$ (E), (4) the large conversion of 12-Cl-1,7-$\mathrm{CHPB_{10}H_9}$ (G) to 7-Cl-1,12-$\mathrm{CHPB_{10}H_9}$ (C), (5) the small yield of H from G, (6) the large percentage of A formed from H, (7) the lack of interconversion between A and C, and (8) the similar yields of B and D from A.

These major trends can then be compared to the predicted yield percentages from the three major mechanisms as listed in Table XI. Once again the only mechanism to predict correctly almost all of these trends as well as the final distribution turns out to be the one involving rotations of pentagonal pyramids. Especially convincing is the lack of interconversion among the two 1,12 isomers A and C; interconversion by the other two mechanisms is predicted to be sizable. Also interesting is the small yield of 9(10)-Cl-1,7- from the 4(6)- and 8(11)-Cl-1,7-$\mathrm{CHPB_{10}H_9}$ isomers, a result only possible in the pathway characterized by the rotating pyramids.

Several alternate mechanisms were also examined for possible correlation with experimental results. The opening of the icosahedron into a nido structure with a pseudo 13-atom cage like the one found for (π-$\mathrm{C_5H_5}$)Co($\mathrm{C_2B_{10}H_{12}}$) and related compounds is a plausible choice.[17-19] Some evidence for the occurrence of this process at high temperatures is suggested by the gas-phase reaction of carborane $\mathrm{C_2B_{10}H_{12}}$ and (π-$\mathrm{C_5H_5}$)Co(CO)$_2$ without first opening the icosahedron by the usual chemical methods.[20] This mechanism, as illustrated in Figure 7A, will then be similar to the one suggested to account for the ready interconversion of (π-$\mathrm{C_5H_5}$)Co(7,9-$\mathrm{C_2B_{10}H_{12}}$) and (π-$\mathrm{C_5H_5}$)Co(7,11-$\mathrm{C_2B_{10}H_{12}}$) in solution,[18] with the transition metal vertex left vacant. Related also is the mechanism of $\mathrm{B_{11}H_{11}}^{2-}$ rearrangement where a vacancy exists

Table XII. Conversions between the Three $CHPB_{10}H_9Cl$ Families Allowed by the Alternate Mechanisms[a]

1,2 into 1,7	1,7 into 1,7	1,7 into 1,12	1,12 into 1,12
	I. Pseudo 13-Atom Nido Intermediate[b]		
12 → 9(10)	2(3) → 4(6), 8(11)	2(3) → 2, 7	2 → 7
	4(6) → 2(3), 5, 8(11), 9(10)	4(6) → 2	7 → 2
	5 → 4(6), 9(10)	5 → 2	
	8(11) → 2(3), 4(6), 9(10), 12	8(11) → 7	
	9(10) → 4(6), 5, 8(11), 12	9(10) → 2, 7	
	12 → 8(11), 9(10)	12 → 7	
	II. Cuboctahedron with Restricted Triangle Rotations[c]		
12 → 9(10), 8(11), 12	2(3) → 4(6), 8(11), 9(10)	2(3) → 2, 7	None
	4(6) → 2(3), 5, 9(10), 8(11)	4(6) → 2	
	5 → 4(6)	5 → 2	
	8(11) → 2(3), 4(6), 9(10), 12	8(11) → 7	
	9(10) → 2(3), 4(6), 8(11)	9(10) → 2, 7	
	12 → 8(11)	12 → 7	
	III. Diamond–Square–Diamond Twist Mechanism		
12 → 9(10)	2(3) → 4(6), 8(11)	2(3) → 2, 7	2 → 7
	4(6) → 2(3), 5, 9(10)	4(6) → 2	7 → 2
	5 → 4(6), 9(10)	5 → 7	
	8(11) → 2(3), 12	8(11) → 7	
	9(10) → 4(6)	9(10) → 2	
	12 → 8(11), 9(10)	12 → 7	

[a] Only the experimentally observed conversions are tabulated. [b] No limitation is placed on the positions of the C or P in the nido structure. [c] Only BBP and BBC triangles are allowed to rotate in the cuboctahedron, no other triangles rotate, and the simple cuboctahedral mechanism is not allowed to occur.

in the intermediate.[21,22] Examination of this mechanism and its allowed transitions gave correct predictions for the 12-Cl-1,2 to 9(10)-Cl-1,7 rearrangement, the 1,7 to 1,12 rearrangement, and some of the inter-1,7 conversions. However, the two major discrepancies are the allowed 2-Cl- and 7-Cl-1,12-$CHPB_{10}H_9$ interconversions and the predicted rearrangements of both 4(6)- and 8(11)-Cl-1,7 isomers into 9(10)-Cl-1,7-$CHPB_{10}H_9$.

Selective triangle rotations in the cuboctahedral intermediate have already been suggested to explain some of the halocarborane isomerization results.[1–3] Restricting these rotations to only BBP and BBC triangles does not markedly improve the poor correlation of the predicted trends with the actual ones (Table XII and Figure 7B).

A diamond–square–diamond twist mechanism (Figure 7C) with the opening of the icosahedron into a single square face followed by a cooperative twisting of the remaining part of the skeleton from the square face can also explain the 12-Cl-1,2- to 9(10)-Cl-1,7-$CHPB_{10}H_9$ rearrangement. The other predictions (Table XII), however, do not match the experimental trends very well (Table X) and this mechanism is therefore not very likely to be significant for the rest of the isomerizations.

While none of these alternate pathways or the other two major mechanisms can be rigorously excluded, the one involving rotation of pentagonal pyramids probably makes a major contribution to the overall process.

More complete labeling of the cage atoms may yield more detail and more complexities in these mechanisms. The "tagging" of only three cage atoms in the present study may have masked these hints of complexity and may not have yielded a complete and detailed picture. We must also comment that it is not entirely unlikely that different mechanisms may dominate consecutive rearrangements and that a variety of combined processes, major and minor, may exist for any single isomerization step. We do conclude from the present study that the substitution of a CH unit by an isoelectronic P atom in an icosahedral cage introduces enough electronic and (or) geometric distortion into the icosahedron to cause a drastic shift in the rearrangement mechanism. Electronic effects due to cage substituents have already been shown to influence the rearrangement process.[2] A trivalent P atom has apparently stabilized the pentagonal-pyramid intermediate relative to the cuboctahedral intermediate. Further systematic studies on icosahedral rearrangements with various heteroatom carboranes should be undertaken in order to elucidate further the nature of these changes.

Acknowledgment. We are indebted to Dr. R. J. Wiersema and C. Salentine of the University of California at Los Angeles for recording the ^{11}B NMR spectra. We also thank the Office of Naval Research for support and Y.-Y. Chiu for helpful suggestions.

Registry No. 2-Cl-1,12-$CHPB_{10}H_9$, 54365-61-6; 2(3)-Cl-1,7-$CHPB_{10}H_9$, 54365-62-7; 7-Cl-1,12-$CHPB_{10}H_9$, 54365-63-8; 4(6)-Cl-1,7-$CHPB_{10}H_9$, 54365-64-9; 5-Cl-1,7-$CHPB_{10}H_9$, 54365-54-7; 8(11)-Cl-1,7-$CHPB_{10}H_9$, 54365-65-0; 12-Cl-1,7-$CHPB_{10}H_9$, 54365-66-1; 9(10)-Cl-1,7-$CHPB_{10}H_9$, 34247-07-9; 4(5)-Cl-1,2-$CHPB_{10}H_9$, 54365-67-2; 7(11)-Cl-1,2-$CHPB_{10}H_9$, 54365-55-8; 8(10)-Cl-1,2-$CHPB_{10}H_9$, 54365-56-9; 9-Cl-1,2-$CHPB_{10}H_9$, 54365-57-0; 12-Cl-1,2-$CHPB_{10}H_9$, 54365-58-1; 1,2-$CHPB_{10}H_{10}$, 30112-97-1; 1,7-$CHPB_{10}H_{10}$, 17398-92-4; 1,12-$CHPB_{10}H_{10}$, 23151-44-2; 9,10-Cl_2-1,7-$CHPB_{10}H_8$, 54365-59-2.

Supplementary Material Available. A listing of structure factor amplitudes will appear following these pages in the microfilm edition of this volume of the journal. Photocopies of the supplementary material from this paper only or microfiche (105 × 148 mm, 24× reduction, negatives) containing all of the supplementary material for the papers in this issue may be obtained from the Journals Department, American Chemical Society, 1155 16th St., N.W., Washington, D.C. 20036. Remit check or money order for $4.50 for photocopy or $2.50 for microfiche, referring to code number AIC40481+.

References and Notes

(1) H. D. Kaesz, R. Bau, H. A. Beall, and W. N. Lipscomb, *J. Am. Chem. Soc.*, **89**, 4218 (1967).
(2) H. V. Hart and W. N. Lipscomb, *J. Am. Chem. Soc.*, **91**, 771 (1969).
(3) H. V. Hart and W. N. Lipscomb, *Inorg. Chem.*, **12**, 2644 (1973).
(4) A. Kaczmarczyk, R. D. Dobrott, and W. N. Lipscomb, *Proc. Natl. Acad. Sci. U.S.A.*, **48**, 729 (1962).
(5) L. I. Zakharkin and V. N. Kalinen, *Dokl. Akad. Nauk SSSR*, **169**, 590 (1966).
(6) D. Grafstein and J. Dvorak, *Inorg. Chem.*, **2**, 1128 (1963).
(7) L. I. Zakharkin and V. I. Kyskin, *Zh. Obshch. Khim.*, **40**, 2234 (1970).
(8) J. Little, J. Morgan, and L. J. Todd, *J. Am. Chem. Soc.*, **89**, 5495 (1967).
(9) C. W. Burnham, *Am. Mineral.*, **51**, 159 (1966). Adapted for use with the Picker diffractometer by C. W. Burnham.
(10) A. D. Rae, *Acta Crystallogr.*, **19**, 683 (1965).
(11) Supplementary material.
(12) A. I. Echeistova, Y. K. Syrkin, L. I. Zakharkin, and V. I. Kyskin, *Zh. Strukt. Khim.*, **11**, 552 (1970).
(13) A. I. Echeistova, Y. K. Syrkin, and L. I. Zakharkin, *Zh. Strukt. Khim.*, **12**, 728 (1971).
(14) L. I. Todd, A. R. Burke, A. R. Garber, H. T. Silverstein, and B. N. Storhoff, *Inorg. Chem.*, **9**, 2175 (1970).
(15) R. Maruca, H. Schroeder, and A. W. Laubengayer, *Inorg. Chem.*, **6**, 572 (1967).
(16) V. Gregor, V. Jehlicka, and J. Stuchlik, *Collect. Czech. Chem. Commun.*, **37**, 3859 (1972).
(17) G. B. Dunks, M. M. McKown, and M. F. Hawthorne, *J. Am. Chem. Soc.*, **93**, 2541 (1971).
(18) D. F. Dustin, G. B. Dunks, and M. F. Hawthorne, *J. Am. Chem. Soc.*, **95**, 1109 (1973).
(19) M. R. Churchill and B. G. DeBoer, *Inorg. Chem.*, **13**, 1411 (1974).
(20) V. N. Miller, L. G. Sneddon, D. C. Beer, and R. N. Grimes, *J. Am. Chem. Soc.*, **96**, 3090 (1974).
(21) W. N. Lipscomb, *Science*, **153**, 373 (1966).
(22) E. I. Tolpin and W. N. Lipscomb, *J. Am. Chem. Soc.*, **95**, 2384 (1973).